

F. KÜHNEMANN^{1,2,✉}
M. WOLFERTZ¹
S. ARNOLD¹
M. LAGEMANN¹
A. POPP¹
G. SCHÜLER²
A. JUX²
W. BOLAND²

Simultaneous online detection of isoprene and isoprene-*d*₂ using infrared photoacoustic spectroscopy

¹ Institute of Applied Physics, Bonn University, Wegelerstr. 8, 53115 Bonn, Germany

² Max Planck Institute of Chemical Ecology, Winzerlaer Str. 10, 07745 Jena, Germany

Received: 3 May 2002/Revised version: 31 May 2002
Published online: 21 August 2002 • © Springer-Verlag 2002

ABSTRACT A photoacoustic spectrometer for the simultaneous detection of isoprene and the deuterated species [4,4-²H]-2-methyl-1,3-butadiene (isoprene-*d*₂) is presented. Using a sealed-off ¹³CO₂ laser a single-component detection limit of 400 ppt (isoprene) and 600 ppt (isoprene-*d*₂) was achieved. Simultaneous monitoring of both compounds allowed the detection of labelling levels down to 6% (isoprene-*d*₂ in total isoprene) with a time resolution of 3 min.

In emission studies with *Eucalyptus globulus*, the deuterated precursor [4,4-²H]-1-deoxy-D-xylulose was fed to a leaf through the transpiration stream. Emission of isoprene-*d*₂ started as early as 10 min after application of the precursor.

PACS 42.55.Lt; 42.62.Be; 82.80.Gk; 33.20.Eq

1 Introduction

Infrared spectroscopic techniques are known to be sensitive tools for trace gas detection. Different methods are used to cover a wide range of applications such as combustion processes and immission control or emissions from anthropogenic or natural sources. Selecting the appropriate method for a special analytical problem depends strongly on the sample conditions (concentrations, volume, temperature, possible interfering species).

In the present case, the task was to simultaneously detect isoprene (2-methyl-1,3-butadiene, C₅H₈), a major volatile organic compound (VOC) emitted by plants [1], and its deuterated isotopomers. Isoprene plays an important role in atmospheric chemistry due to the large amounts emitted into the atmosphere and its high reactivity, especially with HO species [2]. Because of this background there is a strong interest in modelling its emission (especially from deciduous trees) and understanding the regulation of isoprene emission. Identifying the regulatory step in isoprene biosynthesis requires labelling experiments: Isoprene precursors (containing ¹³C or ²H) are fed to the plant and the emission of the respective labelled isoprene is monitored depending on the external conditions of the plant. Isoprene emission may vary on the

time scale of a few minutes. This requires a very fast, preferably continuous detection technique for isoprene and the respective isotopomers.

The established technique for fast isoprene measurement is chemiluminescence, exploiting the fluorescence of formaldehyde which is produced upon reaction of isoprene with ozone [3]. The major advantage of this method is its high sensitivity at the sub-ppb level with less than 1 s time resolution, but the approach completely lacks selectivity for individual isotopomers of isoprene. Other methods with acceptable sensitivity include gas chromatography with different detectors. A survey of such isoprene detection techniques is given in [4].

Mass spectroscopic (MS) techniques have the potential for isotopomer-selective detection. With respect to isoprene, Delwiche and Sharkey used conventional headspace trapping and off-line gas chromatographic analysis with mass spectroscopic detection (GC/MS) to study the incorporation of ¹³C in isoprene formation [5]. Zeidler et al. applied GC/MS to detect deuterium-labelled isoprene after feeding of a deuterated precursor [6]. Automated MS systems have been used for the monitoring of ambient isoprene down to a few parts per trillion (10⁻¹² pt) [7]. Such low concentrations require however a sample pre-concentration, and data acquisition time is in the 10–30 min range.

Proton transfer reaction mass spectrometry is a relatively new technique which allows ppt level detection of isoprene and its isotopomers in the gas flow [8]. Time resolution is only limited by the residence time of the gas in the detector, yielding sampling frequencies of 1 Hz and more.

A different approach to isotopomer-selective trace gas detection for labelling studies is infrared spectroscopy. In this paper we present the first report on a continuous and simultaneous detection of isoprene and its isotopomer isoprene-*d*₂. Monitoring is done using a photoacoustic (PA) spectrometer with a sealed-off CO₂ laser. Photoacoustic spectroscopy has been shown to be a powerful technique for the detection of low trace gas concentrations in small samples [9–12], for example when studying emissions from plants. In a previous paper we had demonstrated that PA detection is a tool for sensitive and fast isoprene detection [4]. The shift of the vibrational frequencies due to isotopic substitution by deuterium changes the spectrum in a characteristic fashion and facilitates a high degree of isotopomer selectivity.

✉ Fax: +49-228/733474, E-mail: frank.kuehnemann@iap.uni-bonn.de

The present paper is organised as follows: The ro-vibrational spectrum of isoprene and isoprene- d_2 is analysed in order to select the most suitable CO_2 laser lines for the detection of both compounds. The principal outline of an optimised spectrometer is described and the performance is discussed. To demonstrate the capabilities of the new spectrometer, physiological experiments using *Eucalyptus globulus* are presented where isoprene- d_2 is synthesised by the plant after feeding of an appropriately labelled precursor.

2 Infrared spectra of isoprene and isoprene- d_2

Isoprene (2-methyl-1,3-butadiene, C_5H_8) and its deuterated isotopomer ([4,4- ^2H]-2-methyl-1,3-butadiene, $\text{C}_5\text{H}_6\text{D}_2$, = isoprene- d_2) display characteristic infrared spectra with ro-vibrational bands in the 3–4, 5–8 and 9–12 μm regions. The rotational structure is not resolved, but the bands show prominent Q -branches, as can be seen from the Fourier transform infrared (FTIR) spectra in Fig. 1 (0.025 cm^{-1} resolution, Bruker Equinox 55). The isoprene spectrum was

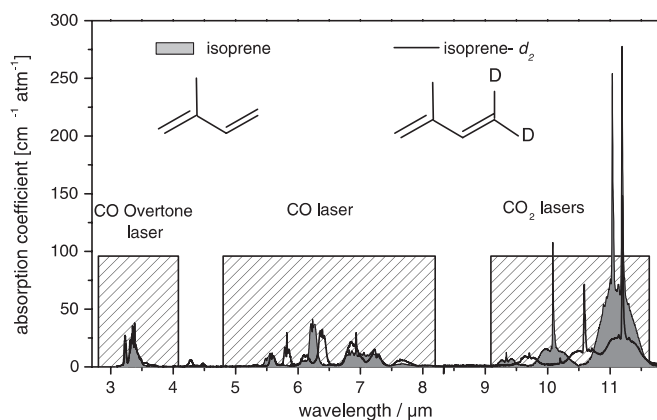


FIGURE 1 FTIR absorption spectra of isoprene (grey area) and isoprene- d_2 (black line) in the 3–11 μm range. The spectra are scaled to 1 atm and 1 cm path length. The boxes indicate the coarse emission ranges of the $^{12}\text{CO}_2$ and $^{13}\text{CO}_2$ lasers, CO and CO overtone lasers, respectively. The symbols show the structure of isoprene and isoprene- d_2 , respectively

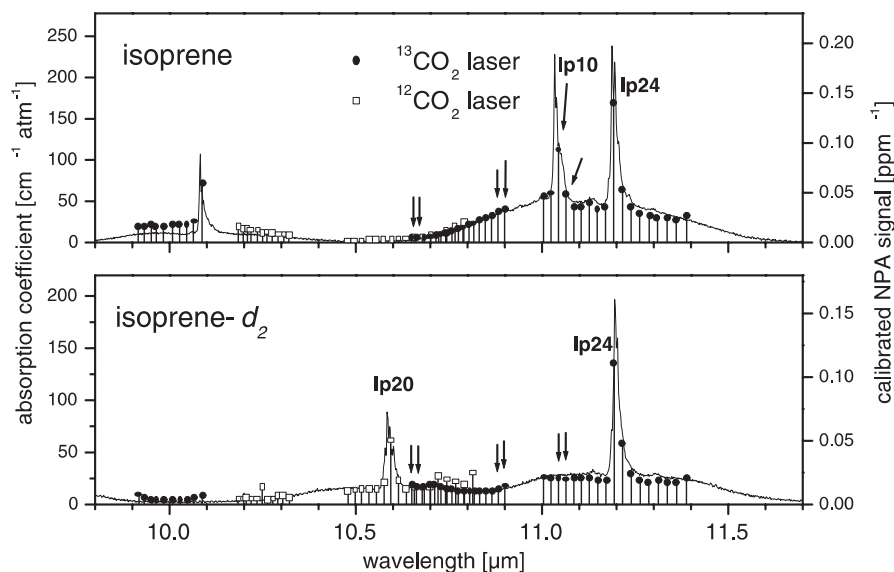


FIGURE 2 FTIR spectra (left axes) of isoprene and isoprene- d_2 in the 9–12 μm range and the PA fingerprint spectra (right axes) of both species measured with the $^{12}\text{CO}_2$ laser (open boxes) and the $^{13}\text{CO}_2$ laser (filled circles). The arrows indicate the laser lines used for the simultaneous detection of both compounds with the $^{13}\text{CO}_2$ laser

recorded from a certified isoprene sample (5% in grade 5 N_2). The isoprene- d_2 spectrum was recorded from evaporated isoprene- d_2 (synthesised according to Gajewski et al. [13]) which was diluted in grade 5 N_2 to give a 2.28% sample. Both absorption spectra were then scaled to 1 atm and 1 cm path length.

The bending vibrations in the 9–12 μm range exhibit the strongest absorption. Figure 2 shows the FTIR spectra for both isotopomers in this range. The strong Q -branches of different vibrational bands promise very good sensitivity and selectivity. Substituting the hydrogen atoms in the unsubstituted vinyl group by deuterium atoms ($-\text{C}=\text{C}^2\text{H}_2$) results in a shift of the frequencies for the associated C–H stretching and bending vibrations. This effect is most clearly seen for the two Q -branches at 11.05 and 11.2 μm . The substitution shifts the 11.05 μm peak towards 14 μm (not shown in the graph), whereas the 11.2 μm peak representing the unlabelled $\text{H}_2\text{C}=\text{C}(\text{CH}_3)$ segment remains unchanged. In this wavelength range the CO_2 laser is the most suitable laser source for PA detection. Since the $^{12}\text{CO}_2$ laser emission only reaches up to 10.85 μm , $^{13}\text{CO}_2$ is required to probe the strong Q -branches around 11 μm . The vertical lines with the symbols indicate the positions of the $^{12}\text{CO}_2$ and $^{13}\text{CO}_2$ laser lines, their heights represent the photoacoustic fingerprint spectra (scaled to 1 ppm), recorded as described in Sect. 3.2. The axes for the PA data have been scaled to the FTIR data.

3 The spectrometer

3.1 Setup

The general setup of the spectrometer is shown in Fig. 3. A home-made sealed-off CO_2 laser was used which could be filled with different laser gas mixtures to operate on $^{12}\text{C}^{16}\text{O}_2$ or $^{13}\text{C}^{16}\text{O}_2$, respectively [14]. The open-structure discharge cell (16 mm inner diameter) was placed in a resonator formed by a curved gold mirror ($r = 10$ m) and a diffraction grating (250 lines/mm) in Littrow configuration. Laser radiation was coupled out of the resonator through the zero-th order of the grating.

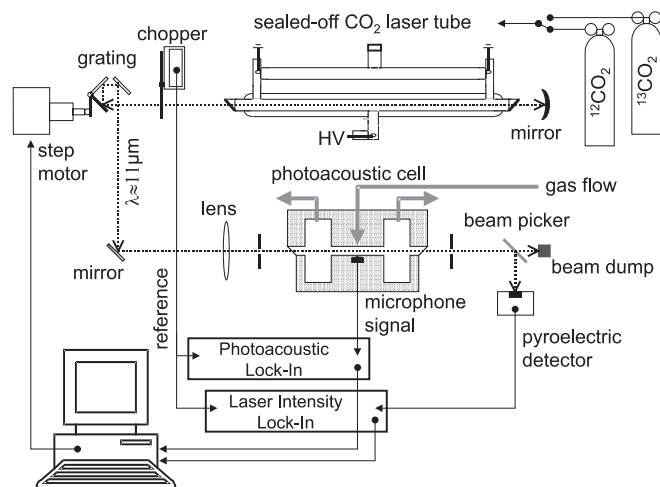


FIGURE 3 Setup of the sealed-off CO₂ laser PA spectrometer

The laser gas mixtures (see Table 1) were prepared in a vessel prior to expansion into the discharge cell to the required total pressure of 16 mbar (¹²CO₂ laser) or 8.5 mbar (¹³CO₂ laser), respectively. High voltage was supplied by a current-stabilised power supply. A two-branch dc discharge was operated with 660 kΩ resistors per branch in series. Laser power up to 600 mW (single mode) was achieved. Intra-cavity pin holes controlled TEM₀₀ operation of the laser. For both CO₂ isotopomers the laser operated on the *P*- and *R*-branches of the I and II bands (see Fig. 4). Amplitude modulation for the photoacoustic detection was achieved with an intra-cavity chopper. The chopping frequency was tuned to the resonance of the PA cell by the computer.

Laser lines were selected by turning the grating with a computer-controlled stepping motor. The calibration procedure has been adapted from the CO₂ laser PA spectrometer dedicated to studies of biogenic ethylene emissions [15]: A complete grating angle scan yields the positions of the intensity peaks (i.e. the laser lines) as a function of the grating angle. To derive an absolute wavelength scale at least a few laser lines across the emission range of the laser have to be assigned. For this purpose characteristic coincidences between the absorption features of suitable gases and individual CO₂ laser lines were used. Table 2 lists the molecules and laser lines which were used to calibrate the present spectrometer. The *I*_{p10} and *I*_{p24} lines of the ¹³CO₂ laser and their isoprene PA signals are marked in Fig. 2, upper panel. The lines were identified from a PA measurement. With their accurately

	¹² CO ₂ mixture	¹³ CO ₂ mixture
¹² CO ₂	10	
¹³ CO ₂		6.8
He	66	64.5
N ₂	11	13.3
CO	8.2	
H ₂	1.2	0.9
Xe	3	4.3
O ₂	0.6	10.2

TABLE 1 Relative partial pressures of the gas components for the laser gas mixtures

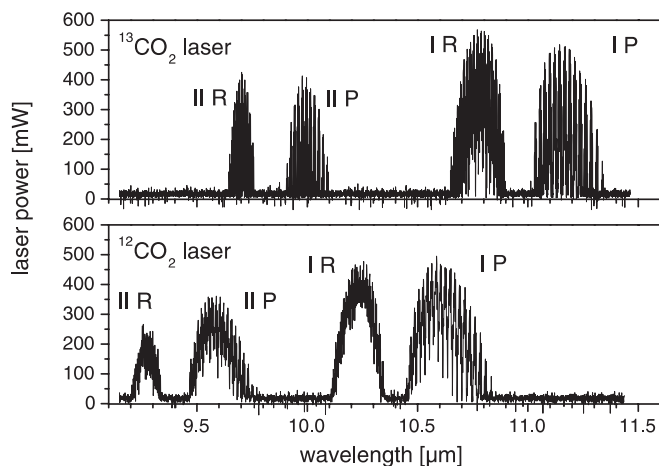


FIGURE 4 Emission spectra of the ¹²CO₂ and ¹³CO₂ lasers used in the experiment. The symbols indicate the *P*- and *R*-branches of the I and II bands of the isotopomers

Molecule	Laser type	Laser line	Line position/cm ⁻¹ [16]
Isoprene	¹³ CO ₂	<i>I</i> _{p24}	893.372
	¹³ CO ₂	<i>I</i> _{p10}	905.4110
Ethylene	¹² CO ₂	<i>I</i> _{p14}	949.4793
	¹² CO ₂	<i>I</i> _{r20}	975.9304

TABLE 2 Gases and laser lines used for the wavelength calibration of the spectrometer

known positions [16] a polynomial fit assigns wavelengths to the grating angle positions. This yields an emission spectrum as in Fig. 4 and allows identification of the remaining laser lines. When a laser line is selected for operation, the computer sets the grating angle according to the stored data. Additional tuning is performed for maximum line intensity and the new optimum angle is stored.

The laser beam was focused into the photoacoustic (PA) cell with a ZnSe lens. The PA cell was made of aluminium with a stainless steel resonator (length 80 mm, inner diameter 14 mm). Buffer volumes ($l = 40$ mm, $r = 50$ mm) supplied an acoustic insulation against noise and parasitic window signals. The cell was closed with ZnSe windows at Brewster angle.

Gas flow through the PA cell (one central injection port into the resonator and two exhaust ports via the buffer volumes) was controlled by mass flow controllers. Air flow up to 10 L/h did not impose additional acoustic noise on the Knowles 3024 electret microphone. The microphone signal was amplified and fed into a lock-in amplifier (Stanford Research SR 830) for phase-sensitive detection. Intensity monitoring for the PA measurements was done with a pyroelectric detector using 4% of the laser radiation reflected off a CaF₂ wedge in order not to damage the detector. The detector signal was recorded with another two-phase lock-in amplifier. All functions of the spectrometer are computer-controlled.

The photoacoustic signal is divided by the laser power yielding amplitude and phase of the normalised photoacoustic (NPA) signal, which is proportional to the trace gas concentration. Trace gas measurements were performed in two different modes: If only one species was present in the carrier gas the laser was permanently operated on a certain laser line and data

were acquired every 3 s (for a lock-in time constant of 1 s). To analyse mixtures, the NPA signal was recorded at a set of laser lines. Tuning the laser to a new line and recording the data took about 30 s. Thus with six laser lines (as in Sect. 3.3) about 3 min were required to generate a new set of concentration data.

3.2 Limit of detection

For one trace gas species in the sample the NPA signal n on a given line is the product of the gas concentration c and the sensitivity A (calibrated NPA signal per ppm) at this laser line. Concentration calibration of the spectrometer was performed by recording the fingerprint spectra for mixtures of isoprene and isoprene- d_2 , respectively, at known concentrations in grade 5 N_2 . For isoprene, a certified mixture of (1.01 ± 0.03) ppm (Praxair, Biebesheim am Rhein) was used. The isoprene- d_2 mixture was prepared from evaporated isoprene- d_2 to a nominal concentration of 1.5 ppm. The mixing uncertainty of 20% was compensated by scaling the NPA signal to a concentration of 1 ppm using the FTIR data for both compounds (see above) and the accurately calibrated isoprene PA fingerprint. In Fig. 2 the PA fingerprints for both species are shown scaled to the FTIR data for comparison.

The individual detection limits for isoprene and isoprene- d_2 were derived by comparing their PA fingerprints with the background signal. The strongest gas signals for both isoprene and isoprene- d_2 were obtained on the I_{p24} line of the $^{13}CO_2$ laser at $11.19 \mu m$ (in coincidence with the Q -branch) with $A_{iso} = 0.14 \text{ ppm}^{-1}$ and $A_{d2} = 0.11 \text{ ppm}^{-1}$, respectively. The background signal was measured when the PA cell was flushed with grade 5 nitrogen, which was additionally cleaned with a liquid nitrogen cooling trap. At the I_{p24} line a value of $(8.35 \pm 0.22) \times 10^{-4}$ for a 1 s lock-in time constant was measured. The amplitude of this signal determined the background equivalent concentration (bec) to be 6 ppb for isoprene and 7.6 ppb for isoprene- d_2 . The high stability of the background signal (which was also maintained in multi-line mode) allowed subtraction of the background from the gas signal. This yielded detection limits (3σ levels) of 400 ppt for isoprene and 600 ppt for isoprene- d_2 at a detection time of 3 s.

The analytical problem addressed in this work was, however, the simultaneous detection of both compounds. The selectivity matter had to be analysed with respect to: i) the simultaneous detection of isoprene and isoprene- d_2 ; and ii) cross-interference due to other trace gases in the sample.

3.3 Isotomer selectivity

From the FTIR spectra and the PA fingerprints (Fig. 2), it is obvious that different features in the spectra of both isoprene isotopomers can be monitored when either the $^{12}CO_2$ or the $^{13}CO_2$ laser are used. With the $^{13}CO_2$ laser (solid circles in Fig. 2) the common strong Q -branch at $11.19 \mu m$ is detected and, in addition, the Q -branch of natural isoprene at $11.05 \mu m$. Furthermore, the two compounds show a different absorption contour in the range of the IR branch (10.62 to $10.8 \mu m$). These characteristics are sufficient for a selective detection of both isoprene isotopomers. To demonstrate this,

gas mixtures were prepared with variable concentrations of isoprene and isoprene- d_2 , respectively, in grade 5 N_2 . Six laser lines in the IP and IR branches of the $^{13}CO_2$ laser were used for the simultaneous detection of both species: I_{p10} , I_{p12} , I_{r8} , I_{r10} , I_{r32} , I_{r34} (indicated with arrows in Fig. 2). The concentrations were determined analysing the PA signals at these six lines with a non-linear least-squares fit as described previously [4, 12], including the removal of the background signal. The results are shown in Fig. 5, demonstrating the good coincidence between the set and the detected concentrations within the experimental uncertainties. In this experiment relatively large isoprene- d_2 concentrations had been chosen. The biological measurement (presented later in Sect. 4) revealed the detection of labelling levels below 10%.

The use of the $^{12}CO_2$ laser (open squares in Fig. 2) gives a different access to the analysis of such mixtures. The I_{p20} line (marked in Fig. 2, lower panel) has a coincidence with the Q -branch of isoprene- d_2 at $10.59 \mu m$. This gave rise to an isoprene- d_2 signal ($A_{d2} = 0.051 \text{ ppm}^{-1}$) which was 16 times stronger than the signal for isoprene ($A_{iso} = 0.0032 \text{ ppm}^{-1}$). Isoprene shows only a broad, general absorption in this band of the $^{12}CO_2$ laser. This will allow the detection of labelling levels down to 5% isoprene- d_2 in natural isoprene.

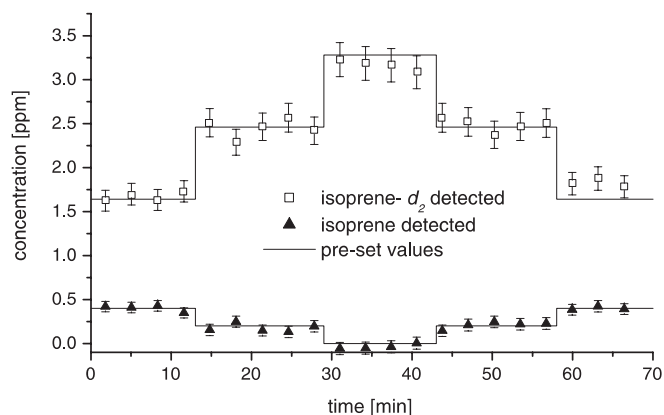


FIGURE 5 Analysis of an isoprene–isoprene- d_2 mixture at different concentrations using the $^{13}CO_2$ laser with six laser lines as indicated in Fig. 2

3.4 Cross-interference to other compounds

In plant physiological emission studies the selectivity has to be ensured, however, even with other absorbing species present in the mixture. In the case of isoprene, competing emissions from plants are primarily carbon dioxide, water and a blend of volatile hydrocarbons (VOCs), especially low-boiling terpenoids. As described previously, a temperature-regulated cooling trap was used to remove the water vapour and most of the VOCs [4]. One of the volatile compounds commonly present in blends emitted from plants is methyl salicylate ($C_8H_8O_3$, MeSa). Figure 6 shows the efficiency of the trap with respect to isoprene and MeSa as a function of trap temperature. In this experiment, premixed samples of 1 ppm isoprene and 3 ppm MeSa, respectively, in grade 5 nitrogen were flown through the cooling trap and the concentrations downstream of the trap were measured with the PA spectrometer. MeSa was efficiently removed from the gas flow

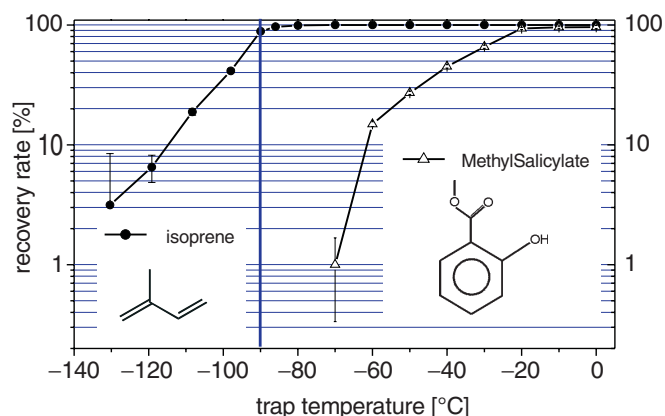


FIGURE 6 Temperature-dependent transmission (recovery rate) through the cooling trap for 1 ppm isoprene and 3 ppm methyl salicylate, respectively. The vertical line indicates the working point for the cooling trap in the later experiments

at -90°C and did not contribute to the PA signal anymore whereas isoprene was recovered.

The situation is more complex with carbon dioxide in the sample. In certain experiments the air supplied to the plant was enriched in CO_2 up to levels between 500 and 1000 ppm, which was then partly taken up by the plant. Such CO_2 levels passed the cooling trap at -90°C and gave rise to a strong PA signal when the $^{12}\text{CO}_2$ laser was used. The CO_2 PA signal shows a 180° phase shift relative to the 'normal' gas signals due to the kinetic cooling effect [17]. At the I_{p20} line 1000 ppm CO_2 caused a large PA signal amplitude equivalent to approximately 1 ppm isoprene- d_2 or 16 ppm natural isoprene. This was accounted for by including CO_2 into the fit of the gas concentrations. Experience did show, however, that under conditions of strong CO_2 contributions dominating the PA signals, the determination of native isoprene concentration became less reliable, especially against a strongly changing background of CO_2 in the mixture.

Under these conditions the following biological studies were carried out with the $^{13}\text{CO}_2$ laser. Due to the low abundance of $^{13}\text{CO}_2$ in ambient air ($^{13}\text{C} : ^{12}\text{C} = 0.011$), the CO_2 NPA signal was about 100 times weaker than with the $^{12}\text{CO}_2$ laser and had less weight in the multi-line fit.

3.5 Time resolution

The time resolution of the isoprene detection depends on the gas exchange time in the resonator of the PA cell and on the number of laser lines which are used to determine the gas concentrations in a multi-line fit. At a flow rate of 6 L/h the resonator volume of 12 cm^3 is exchanged once within 7 s. Data acquisition times are 3 s in single-line mode and 30 s per line in multi-line mode.

In plant physiological experiments the time resolution is determined by the gas exchange time for the plant chamber. In the experiments described below, a 350 cm^3 chamber is flushed with air at 6 L/h. To estimate the time resolution the emission of isoprene from the plant was simulated: The chamber was flushed with N_2 at 6 L/h. An isoprene/ N_2 mixture was added to the N_2 flow in the plant chamber keeping the total flow constant. The isoprene signal in the PA

cell started to increase about 1 min after the addition of the gas. This delay was due to the transfer time of the gas through the tubing and the cooling trap into the PA cell. The signal increased to the steady state value in a single-exponential fashion with a time constant $\tau = 220\text{ s}$. Turning off the isoprene flow resulted in a decay of the isoprene signal with a delay of 100 s and a time constant of $\tau = 280\text{ s}$. The difference may be due to a temporarily higher flow rate upon isoprene addition and a reduction of the flow rate upon turning-off.

Higher time resolution may easily be achieved with a faster gas exchange in the plant chamber. The limit will then be set by the number of laser lines required for a multi-gas data analysis, for instance 3 min for six lines.

4 Physiological experiments

In order to demonstrate the scope and capabilities of the spectrometer, preliminary experiments are presented addressing isoprene biosynthesis from exogenously added and deuterium-labelled deoxy-D-xylulose. The measurements were performed with the $^{13}\text{CO}_2$ laser using six laser lines as described above.

4.1 Materials

An *Eucalyptus globulus* tree (about 4 m high) was held in a greenhouse during winter and outdoor during the rest of the year. For the present experiments branches were cut in the greenhouse and transferred into the lab, where they were held under room light and 24°C for up to 4 h until the experiment. Leaves of about 25 cm^2 were cut at the petiole with a razor blade and placed in a vial with water inside the leaf cuvette (350 cm^3). Access to the leaf cuvette for applications was possible through a teflon-coated diaphragm with a syringe, thus avoiding input of ambient air during the measurements.

The leaf was supplied with hydrocarbon-free air at 6 L/h. Downstream from the leaf cuvette, the air passed the cooling trap at -90°C prior to entering the PA spectrometer for analysis. Light was supplied from a 500 W halogen lamp delivering photosynthetic active radiation (PAR) up to $1500\text{ }\mu\text{mol photons cm}^{-2}\text{ s}^{-1}$. Radiation was measured with a EGM-1 detector head (PP systems, UK). The leaf cuvette was placed in a water bath for temperature stabilisation ($\pm 0.3^{\circ}\text{C}$) and removal of the strong infrared radiation from the lamp. Cuvette air temperature was measured with a Pt100 temperature sensor.

4.2 Labelling

One of the intermediate compounds in isoprene synthesis is 1-deoxy-D-xylulose-5-phosphate (DOXP) [18]. The deuterium-labelled free form, [4,4- ^2H]-1-deoxy-D-xylulose (DOX- d_2), was found to be efficiently channelled into terpenoid metabolism. DOX- d_2 was synthesised according to [19, 20]. Solutions at 1 mg/mL were stored at -18°C until use. For the application the water level in the vial was reduced without interruption of the transpiration stream and DOX- d_2 solution was added to the required final concentration.

4.3 Resolution of isoprene detection

Isoprene emission of plants depends on light, temperature and CO_2 concentration and is controlled by enzyme availability, enzyme activity, energy and substrate availability [21, 22]. Due to the strong temperature dependence even minor temperature fluctuations have a significant impact on the isoprene emission rate. Figure 7 shows such an experiment in order to demonstrate the resolution of isoprene measurements. Air temperature in the chamber was oscillating around the set point by $\pm 0.4^\circ\text{C}$ with a period of about 17 min. With the same period oscillations in the isoprene concentration of ± 3 ppb around 225 ppb were observed. This corresponds to a resolution in isoprene detection of 2%. The observed time delay between the temperature peaks and the measured isoprene concentration peaks in the PA cell (approximately 6 min) was mostly due to the gas exchange time in the measurement system at a flow rate of 6 L/h (as discussed in Sect. 3.5). Increasing the air flow rate will reduce the time delay and allow to follow such fast emission rate changes even closer.

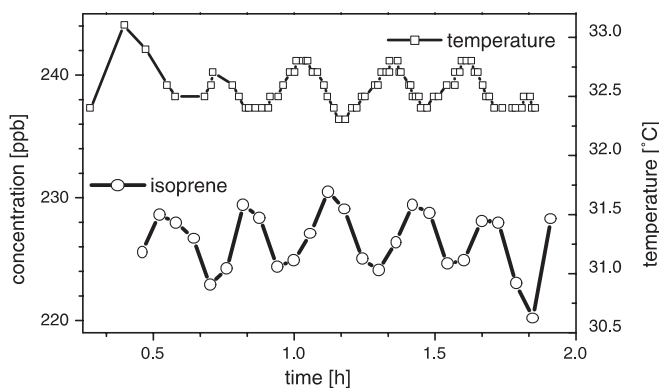


FIGURE 7 Isoprene emission (open circles) from a single *Eucalyptus globulus* leaf is modulated by small-amplitude temperature oscillations (open boxes). The observed time delay between temperature modulation and measured isoprene concentration is mostly due to the gas exchange rate in the leaf chamber and the gas transport as described in the text

4.4 Detection of biogenic isoprene- d_2 emission

The central question was whether or not isoprene- d_2 emitted from a plant after supply with $\text{DOX-}d_2$ can be detected in the presence of natural isoprene. In order to be channelled into the biosynthetic pathway, $\text{DOX-}d_2$ has to be transported into the chloroplast and phosphorylated. Figure 8 shows an example for such a measurement. Isoprene and isoprene- d_2 concentrations are displayed together with the temperature in the leaf cuvette. Prior to the addition of $\text{DOX-}d_2$ the light was turned off for 35 min (grey-shaded box) to characterise the isoprene emission behaviour of the leaf. The observed decay and increase of the isoprene emission is in agreement with the known light dependence of isoprene emission. When isoprene emission had reached the steady state again, $\text{DOX-}d_2$ was applied to the leaf as described above. isoprene- d_2 appeared in the air flow after about 10 min. The fast incorporation is in strong contrast to difficulties observed when a methylated form of DOX was fed to the plant [6]: In that case labelled isoprene was observed only after several

hours of incubation, since the compound had to be hydrolysed before entering the isoprene biosynthetic pathway.

The data in Fig. 8 also demonstrate the reliability of the simultaneous isoprene/isoprene- d_2 detection: When $\text{DOX-}d_2$ was added, the appearance of isoprene- d_2 could be discriminated from the background at concentrations as low as 40 ppb, equivalent to a labelling level of 6% at a total isoprene amount of 600 ppb. The transient isoprene- d_2 signals prior to the $\text{DOX-}d_2$ addition are a cross-talk in the fit when very steep changes in isoprene emission occur (here upon light off and on). This will be omitted in an improved version of the data analysis.

Simultaneously with the increase in isoprene- d_2 emission the production of native isoprene decreased. This effect was observed in all experiments, but to a varying extent, resulting in either a decreasing, increasing or constant sum of total isoprene (natural isoprene plus isoprene- d_2). One example has been chosen here just to demonstrate the capabilities of the new isoprene detection spectrometer. One may expect that the labelling level depends on the photosynthetic capacity and the carbohydrate status of the leaf. The physiological processes behind the labelling are currently under intense investigation.

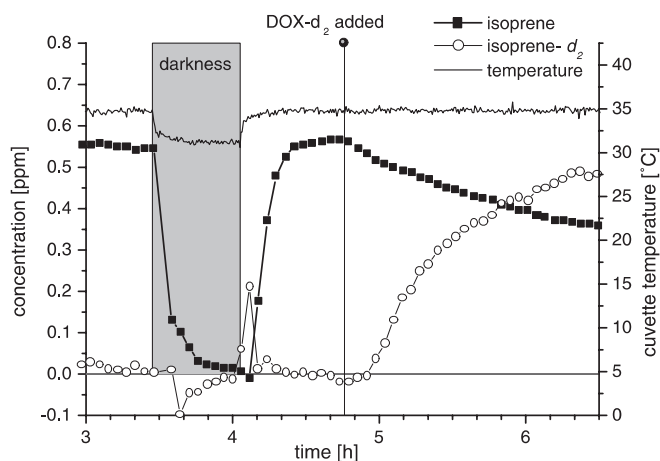


FIGURE 8 Emission of isoprene and isoprene- d_2 by an *Eucalyptus globulus* leaf. Emission of native isoprene (solid boxes) decays to zero during darkness (grey shaded area) and resumes upon light-on. Isoprene- d_2 (open circles) emission starts upon feeding with $\text{DOX-}d_2$ (solid vertical line)

5 Summary

A photoacoustic spectrometer based on a sealed-off $^{13}\text{CO}_2$ laser has been used for the first time to simultaneously detect isoprene and one of its deuterated isotopomers emitted from plants. The time resolution and sensitivity of the instrument perfectly match all requirements to study biogenic isoprene emission. The selectivity allows the detection of minor amounts of labelled material against a large background of natural isoprene, thus qualifying the methodology for physiological studies. The spectrum of isoprene in the 9–12 μm region is well structured with pronounced Q -branches of different ro-vibrational bands. This makes it an ideal candidate for the inclusion of other deuterated isotopomers into the analysis, as they may possibly be produced by the plant upon

feeding of the respective precursors into the pathway of isoprene synthesis. In addition, use of other CO₂ isotopomers as laser gas may further improve the selectivity of the detection.

The physiological experiments did reveal, for the first time, the immediate incorporation of the applied precursor into the biosynthetic pathway and the onset of isoprene-*d*₂ emission within 10 min of application.

ACKNOWLEDGEMENTS The authors thank M. Blanke, Bonn, for providing the EGM detector system. We thank the reviewers for critical comments leading to an improved manuscript.

REFERENCES

- 1 A.B. Guenther: *J. Geophys. Res.* **100**, 8873 (1995)
- 2 F. Fehsenfeld, J. Calvert, R. Fall, P. Goldan, A.B. Guenther, C.N. Hewitt, B. Lamb, S. Liu, M. Trainer, H. Westberg, P. Zimmerman: *Global Biochem. Cycl.* **6**, 389 (1992)
- 3 A.J. Hills, P.R. Zimmerman: *Anal. Chem.* **62**, 1055 (1990)
- 4 H. Dahnke, J. Kahl, G. Schüler, W. Boland, W. Urban, F. Kühnemann: *Appl. Phys. B* **70**, 275 (2000)
- 5 C.F. Delwiche, T.D. Sharkey: *Plant Cell Environ.* **16**, 587 (1993)
- 6 J.G. Zeidler, H.G. Lichtenthaler, H.U. May, F.W. Lichtenthaler: *Z. Naturforsch. C* **52**, 15 (1997)
- 7 D.J. Barket Jr., J.M. Hurst, T.L. Couch, A. Colorado, P.B. Shepson, D.D. Riemer, A.J. Hills, E.C. Apel, R. Hafer, B.K. Lamb, H.H. Westberg, C.T. Farmer, E.R. Stabenau, R.G. Zika: *J. Geophys. Res.* **106**, 24301 (2001)
- 8 W. Lindinger, R. Fall, T.G. Karl: *Adv. Gas Phase Ion Chem.* **4**, 1 (2001)
- 9 F.J.M. Harren, J. Reuss: In: *Encyclopedia of Applied Physics*, Vol. 19 (VCH Publishers, New York 1997) p. 413
- 10 J. Oomens, H. Zuckermann, S. Persijn, D.H. Parker, F.J.M. Harren: *Appl. Phys. B* **67**, 459 (1998)
- 11 M. Nägele, M.W. Sigrist: *Appl. Phys. B* **70**, 895 (2000)
- 12 A.A.E. Martis, S. Büscher, F. Kühnemann, W. Urban: *Instrum. Sci. Technol.* **26**, 177 (1998)
- 13 J.J. Gajewski, K.B. Peterson, J.R. Kagel: *J. Am. Chem. Soc.* **109**, 5545 (1987)
- 14 A. Dax: Ph.D. thesis, Bonn University (1992)
- 15 T. Fink, S. Büscher, R. Gäbler, Q. Yu, A. Dax, W. Urban: *Rev. Sci. Instrum.* **67**, 4000 (1996); T. Fink: Ph.D. thesis, Bonn University (1994)
- 16 W.J. Witteman: *The CO₂ Laser* (Springer-Verlag, Berlin, Heidelberg 1987)
- 17 M. Hammerich, A. Olafsson, J. Henningsen: *Chem. Phys.* **163**, 173 (1992)
- 18 M. Rohmer, M. Knani, P. Simonin, B. Sutter, H. Sahn: *Biochem. J.* **295**, 517 (1993)
- 19 J. Piel, W. Boland: *Tetrahedron Lett.* **38**, 6387 (1997)
- 20 A. Jux, W. Boland: *Tetrahedron Lett.* **40**, 6913 (1999)
- 21 A.B. Guenther, R.K. Monson, R. Fall: *J. Geophys. Res.* **98**, 2839 (1991)
- 22 E.L. Singsaas, T.D. Sharkey: *Plant Cell Environ.* **21**, 1181 (1998)